Where is the string limit in QCD?*

K.J. Juge, J. Kuti, and C.J. Morningstar[a]

[a]Dept. of Physics, University of California at San Diego, La Jolla, California 92093-0319

The energies of glue in the presence of a static quark-antiquark pair are calculated for separations r ranging from 0.1 fm to 4 fm and for various quark-antiquark orientations on the lattice. Our simulations use an improved gauge-field action on anisotropic space-time lattices. Discretization errors and finite volume effects are studied. We find that the spectrum does not exhibit the expected onset of the universal π/r Goldstone excitations of the effective QCD string, even for r as large as 4 fm. Our results cast serious doubts on the validity of treating glue in terms of a fluctuating string for r below 2 fm. Retardation effects in the Υ system are also studied by comparing level splittings from the Born-Oppenheimer approximation with those directly obtained in simulations.

1. Introduction

Accurate knowledge of the properties of the stationary states of glue in the presence of the simplest of color sources, that of a static quark and antiquark separated by some distance r, is an important stepping stone on the way to understanding confinement. It is generally believed that at large r, the linearly-growing ground-state energy of the glue is the manifestation of the confining flux whose fluctuations can be described in terms of an effective string theory. The lowest-lying excitations are then the Goldstone modes associated with spontaneously-broken transverse translational symmetry. Expectations are less clear for small r.

Even the simplest property, the energy spectrum, of the stationary states of glue interacting with a static quark-antiquark pair is not accurately known. The main goal of this work is to remedy this. Here, we present, for the first time, a comprehensive determination of the low-lying spectrum of gluonic excitations in the presence of a static quark-antiquark pair. In this initial study, the effects of light quark-antiquark pair creation are ignored. A few of the energy levels for r less than 1 fm have been studied before[1]. Our results for these quantities have significantly improved precision, and we have extended the range in r to 4 fm. Most of the energy levels presented here have never been studied before. Some of our results were previously reported[2].

The determination of the energies of glue in the presence of a static quark-antiquark pair is also the first step in the Born-Oppenheimer treatment of conventional and hybrid heavy-quark mesons[3]. The validity of the Born-Oppenheimer expansion depends, in part, on the smallness of retardation effects. In order to quantify such effects for the first time, mass splittings for various conventional and hybrid heavy-quark mesons obtained from the leading Born-Oppenheimer approximation are compared to those determined in simulations in which the heavy quark propagates according to a spin-independent nonrelativistic action.

2. Computation of the glue energies

We adopt the standard notation from the physics of diatomic molecules and use Λ to denote the magnitude of the eigenvalue of the projection $\vec{J}_g \cdot \hat{\mathbf{r}}$ of the total angular momentum $\vec{J}_g$ of the gluons onto the molecular axis $\hat{\mathbf{r}}$. The capital Greek letters $\Sigma, \Pi, \Delta, \Phi, \ldots$ are used to indicate states with $\Lambda = 0, 1, 2, 3, \ldots$, respectively. The combined operations of charge conjugation and spatial inversion about the midpoint between the quark and the antiquark is also a symmetry and its eigenvalue is denoted by η_{CP}. States with $\eta_{CP} = 1(-1)$ are denoted by the subscripts g (u). There is an additional label for the Σ states; Σ

*Talk presented by C. Morningstar and poster presented by K.J. Juge.

Table 1
Simulation parameters, including the coupling β, input aspect ratio ξ, lattice size, and the spatial link smearing parameters ζ and n_ζ. The approximate lattice spacings a_s, calculated assuming $r_0^{-1} = 410$ MeV, are also given.

Run	a_s (fm)	β	ξ	Lattice	(ζ, n_ζ)
A	0.29	2.1	8	$(10^2 \times 20) \times 80$	(0.07, 12)
					(0.10, 12)
					(0.15, 12)
B	0.29	2.1	8	$(10^2 \times 20) \times 80$	(0.10, 12)
C	0.29	2.1	8	$14^3 \times 56$	(0.15, 6)
					(0.10, 12)
D	0.27	2.2	5	$12^3 \times 48$	(0.10, 4)
					(0.20, 4)
					(0.30, 4)
E	0.22	2.4	5	$14^3 \times 56$	(0.10, 8)
					(0.15, 8)
					(0.25, 8)
					(0.30, 8)
F	0.19	2.5	5	$(10^2 \times 25) \times 60$	(0.10, 12)
					(0.18, 12)
					(0.26, 12)
G	0.19	2.6	3	$10^3 \times 30$	(0.15, 8)
					(0.30, 8)
H	0.12	3.0	3	$15^3 \times 45$	(0.15, 24)
					(0.22, 24)

states which are even (odd) under a reflection in a plane containing the molecular axis are denoted by a superscript + (−). Hence, the low-lying levels are labelled Σ_g^+, Σ_g^-, Σ_u^+, Σ_u^-, Π_g, Π_u, Δ_g, Δ_u, and so on. For convenience, we use Γ to denote these labels in general.

The glue energies $E_\Gamma(\vec{r})$ were extracted from Monte Carlo estimates of generalized Wilson loops. Recall that the well-known static potential $E_{\Sigma_g^+}(r)$ can be obtained from the large-t behaviour $\exp[-tE_{\Sigma_g^+}(r)]$ of the Wilson loop for a rectangle of spatial length r and temporal extent t. In order to determine the lowest energy in the Γ sector, each of the two spatial segments of the $r \times t$ rectangular Wilson loop must be replaced by a *sum* of spatial paths, all sharing the same starting and terminating sites, which transforms as Γ under all symmetry operations. The easiest way to do this is to start with a single path $\mathcal{P}_\alpha$, such as a staple, and apply the Γ projection operator which is a weighted sum over all symmetry operations; this yields a single gluon operator in the Γ channel. Different gluon operators correspond to different starting paths $\mathcal{P}_\alpha$. Using several (typically 3 to 22) different such operators then produces a matrix of Wilson loop correlators $W_\Gamma^{ij}(r,t)$.

Monte Carlo estimates of the $W_\Gamma^{ij}(r,t)$ matrices were obtained in eight simulations performed on a DEC AlphaStation 500/333 using an improved gauge-field action[4]. The couplings β, input aspect ratios ξ, and lattice sizes for each simulation are listed in Table 1. Our use of anisotropic lattices in which the temporal lattice spacing a_t was much smaller than the spatial spacing a_s was crucial for resolving the glue spectrum, particularly for large r. The couplings in the action depend not only on the QCD coupling β, but also on two others parameters: the mean temporal link u_t and the mean spatial link u_s. Following Ref. [4], we set $u_t = 1$ and obtain u_s from the spatial plaquette. We use $a_s/a_t = \xi$, the input or bare anisotropy, in all of our calculations, accepting the small radiative corrections to the anisotropy as finite lattice spacing errors which vanish in the continuum limit.

To hasten the onset of asymptotic behaviour, iteratively-smeared spatial links[4] were used in the generalized Wilson loops. A single-link procedure was used in which each spatial link variable $U_j(x)$ on the lattice is mapped into itself plus a sum of its four neighbouring (spatial) staples multiplied by a weighting factor ζ. The resulting matrix is then projected back into SU(3). This mapping is then applied recursively n_ζ times, forming new smeared links out of the previously-obtained smeared links. The (ζ, n_ζ) smearing schemes used in the simulations are given in Table 1. Separate measurements were taken for each smearing; cross correlations were not determined. The temporal segments in the Wilson loops were constructed from thermally-averaged links, whenever possible, to reduce statistical noise.

Results for several values of the lattice spacing

were obtained. Our coarsest lattice ($a_s \sim 0.29$ fm) was used in runs A, B, and C in order to probe very large quark-antiquark separations. A large aspect ratio ($\xi = 8$) was needed in order to adequately resolve the correlation functions. In run A, only on-axis measurements were made. Run B was done to reduce uncertainties for the large $r/a_s \geq 9$ measurements. To verify the restoration of rotational symmetry and to rule out problems associated with the roughening transition, off-axis $(r, r, r)/\sqrt{3}$ measurements were made in run C. Agreement of energies obtained using different quark-antiquark orientations on the lattice also helped identify the continuum Λ value corresponding to each level (there are only discrete symmetries on the lattice). Runs D, E, F, and G provided results for different lattice spacings $a_s \sim 0.27, 0.22, 0.19$, and 0.19 fm, respectively. Only on-axis measurements were made in these runs. Runs F and G correspond to the same spatial lattice spacing a_s, but have very different temporal spacings a_t. This provided us with a measure of the a_t^2 errors in our results (our action has $O(a_t^2, a_s^4)$ errors). Such information is important for carrying out the $a_s \to 0$ extrapolations. Run H provided fine-grained ($a_s \sim 0.12$ fm) measurements to assist the continuum-limit extrapolations of the Σ_g^+ and Π_u potentials and was useful for verifying the negligible size of quantum corrections to the lattice anisotropy. To check the anisotropy, the potentials were measured for the quark-antiquark axis taken along the very fine-grained direction and one of the coarser axes was used as the direction of evolution for the system. This run was also important for resolving a slight discrepancy between our Π_u results and those[1,5] obtained using the simple Wilson action at $\beta = 6.0$.

The matrices $W_\Gamma^{ij}(r, t)$ were reduced in the data fitting phase to single correlators and 2×2 correlation matrices using the variational method. The lowest-lying glue energies were then extracted from these reduced correlators by fitting a single exponential and a sum of two exponentials, the expected asymptotic forms, in various ranges $t_{\min}$ to $t_{\max}$ of the source-sink separation. The two-exponential fits were used to check for consistency with the single-exponential fits, and in cases of favourable statistics, to extract the first-excited state energy in a given channel.

Three additional runs on small lattices were done to verify that finite-volume errors in our results were negligible. We confirmed the smallness of the a_s/a_t renormalization for two values of the QCD coupling by extracting the ground state potential from Wilson loops in different orientations. The hadronic scale parameter $r_0 \approx 0.5$ fm was used to determine the lattice spacing[4]. The additive ultraviolet-divergent self-energies of the static sources were removed by expressing all of our results with respect to $\Sigma_g^+(r_0)$. Finite-lattice spacing errors were removed by extrapolating our simulation results for $r_0[E_\Gamma(r) - E_{\Sigma_g^+}(r_0)]$ to the continuum limit. These extrapolations were carried out by fitting all of our simulation results to an ansatz $F_{\rm cont}(r) + a_s^4\, F_{\rm latt}(r)$: a ratio of a polynomial of degree $p+1$ over a polynomial of degree p, where $p = 1$ or 2, was found to work well for the continuum limit form $F_{\rm cont}(r)$, and $F_{\rm latt}(r)$ was chosen empirically to be a sum of three terms $1/\sqrt{r}$, $1/r$, and $1/r^2$. All fits yielded χ^2/dof near unity. Continuum Λ values were easily identified in all cases but one: we were unable to distinguish between a Π_u' and Φ_u interpretation for the on-axis E_u' level.

3. Results

Our continuum-limit extrapolations are shown in Fig. 1. The ground state Σ_g^+ is the familiar static-quark potential. A linearly-rising behaviour dominates the Σ_g^+ potential once r exceeds about 0.5 fm and we find no deviations from the linear form up to 4 fm. The lowest-lying excitation is the Π_u. There is definite evidence of a band structure at large r: the $\Sigma_g^{+\prime}$, Π_g, and Δ_g form the first band above the Π_u; the Σ_u^+, Σ_u^-, Π_u'/Φ_u, and Δ_u form another band. The Σ_g^- is the highest level at large r. This band structure breaks down as r decreases below 2 fm. In particular, two levels, the Σ_g^- and Σ_u^-, drop far below their large-r partners as r becomes small. Note that for r above 0.5 fm, all of the excitations shown are stable with respect to glueball decay. As r decreases below 0.5 fm, the excited levels eventually become unstable as their gaps above

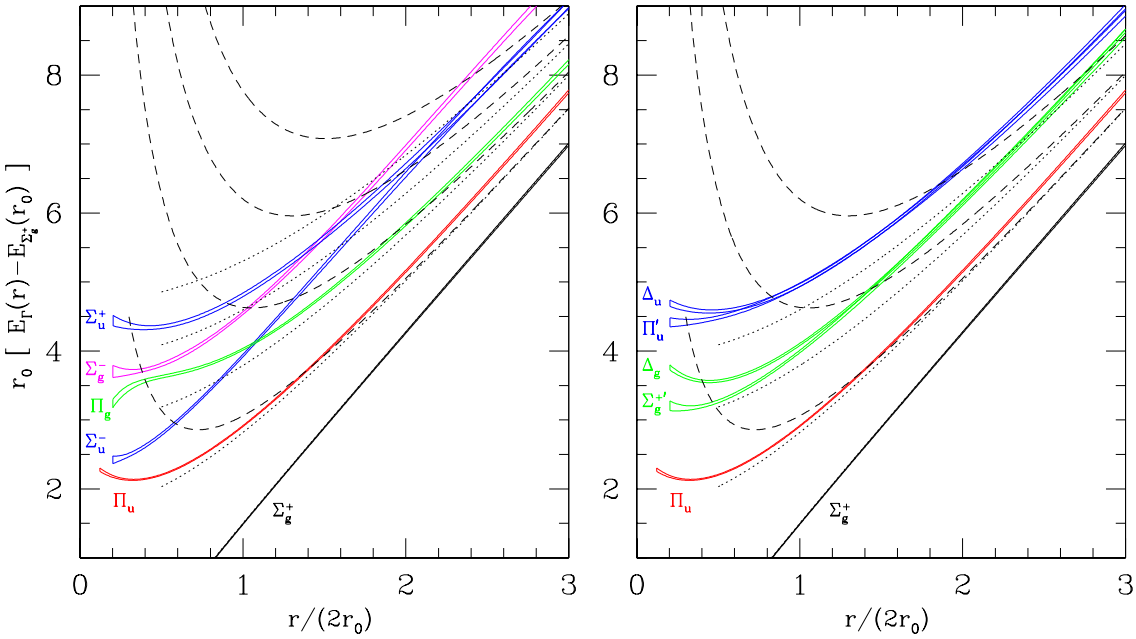

Figure 1. Continuum-limit extrapolations (with uncertainties as indicated) for $r_0[E_\Gamma(r) - E_{\Sigma_g^+}(r_0)]$ against $r/(2r_0)$ for various Γ. The dashed lines indicate the locations of the $m\pi/r$ gaps above the Σ_g^+ curve for $m = 1$, 2, 3, and 4. The dotted curves are the naive Nambu-Goto energies in four-dimensions. Note that we cannot rule out a Φ_u interpretation for the curve labelled Π'_u.

the ground state Σ_g^+ exceed the mass of the lightest glueball.

A feature of any low-energy description of a fluctuating flux tube is the presence of Goldstone excitations associated with the spontaneously-broken transverse translational symmetry. These transverse modes have energy separations above the ground state given by multiples of π/r (for fixed ends). The level orderings and approximate degeneracies of the gluon energies at large r match, without exception, those expected of the Goldstone modes. However, the precise $m\pi/r$ gap behaviour is not observed, as shown in Fig. 2. The energy differences $r_0[E_\Gamma(r) - E_{\Sigma_g^+}(r)]$ for $\Gamma = \Pi_u$, Π_g, Σ_u^-, and Σ_g^- are shown in this figure, along with their expected Goldstone mode behaviours, indicated by the dashed curves. For separations less than 2 fm, one sees from Fig. 1 that the gluon energies lie well below the Goldstone energies and the Goldstone degeneracies are no longer observed. The two Σ^- states are in violent disagreement with expectations from a fluctuating string. Note also that our results clearly disagree with the energies of a Nambu-Goto string naively (ignoring quantization difficulties) determined in four continuous space-time dimensions.

These results are rather surprising and cast serious doubts on the validity of treating glue in terms of a fluctuating string for quark-antiquark separations less than 2 fm. Note that such a conclusion does not contradict the fact that the $\Sigma_g^+(r)$ energy rises linearly for r as small as 0.5 fm. A linearly-rising term is not necessarily indicative of a string: for example, the adiabatic bag model predicts a linearly-rising ground state much before the onset of string-like behaviour, even in the spherical approximation[3]. For r greater than 2 fm, there are some tantalizing signatures of Goldstone mode formation, yet significant disagreements still remain. To what degree these discrepancies can be explained in terms of a distortion of the Goldstone mode spectrum aris-

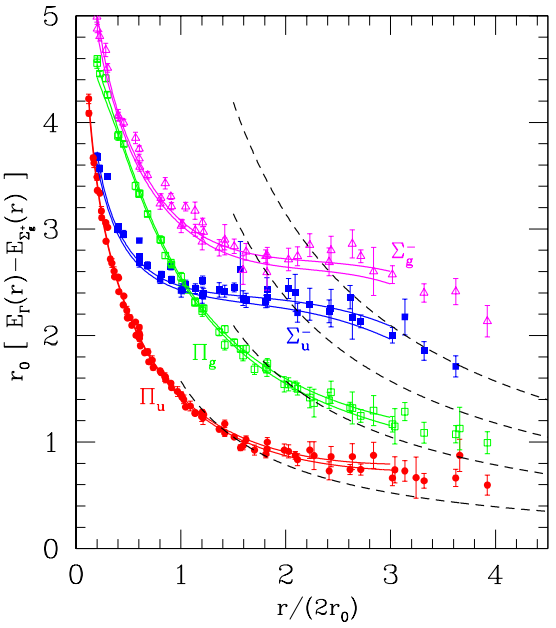

Figure 2. Plot of the energy differences $r_0[E_\Gamma(r) - E_{\Sigma_g^+}(r)]$ against $r/(2r_0)$ for $\Gamma = \Pi_u$, Π_g, Σ_u^-, and Σ_g^-. Results from all of the simulations are shown; the different symbols correspond to the different Γ channels. The pairs of solid curves indicate the continuum-limit extrapolations. The dashed lines show the locations of the $m\pi/r$ excitation gaps for $m = 1$, 2, 3, and 4.

ing from the spatial fixation of the quark and antiquark sources (clamping effect) is currently under investigation. This clamping effect can be confirmed by comparing our results with the excitation spectrum of a closed flux in a periodic box in which this effect is absent. We also plan to study the $SU(2)$ gluon excitation spectrum in order to ascertain how much of the spectrum is independent of the gauge group. Note that it is very unlikely that the transverse extents of our lattices are causing the discrepancies with the Goldstone spectrum[6]. Results for all r up to 4 fm were insensitive to changes in the transverse size from 0.9 to 3 fm. As an added check, we also calculated the wave functions for the first five Fourier modes of the naive Nambu-Goto string; we found that for $r \sim 4$ fm, the widths of these wave functions did not appreciably exceed 1 fm.

4. Hybrid quarkonium

Another reason for studying the energies of glue in the presence of a quark-antiquark pair is the likelihood that these energies will provide insight into the nature of hybrid mesons. The study of hybrid mesons comprised of heavy quarks is the natural starting point in the quest for such an understanding. A great advantage in studying heavy hybrid quarkonium is that such systems can be studied not only by direct numerical simulation, but also using the Born-Oppenheimer expansion. In this approach, the hybrid meson is treated analogous to a diatomic molecule: the slow heavy quarks correspond to the nuclei and the fast gluon field corresponds to the electrons[3]. The first step in the Born-Oppenheimer treatment is to determine the energy levels of the glue (and light quark-antiquark pairs) as a function of the heavy quark-antiquark separation, treating the heavy quark and antiquark simply as spatially-fixed color sources. Each such energy level defines an adiabatic potential. The quark motion is then restored by solving the nonrelativistic Schrödinger equation using these potentials. Conventional quarkonia arise from the lowest-lying potential; hybrid quarkonium states emerge from the excited potentials.

Once the gluon energies are determined, the Born-Oppenheimer approach yields the entire leading-order spectrum very easily, in contrast to direct simulations. However, the validity of the Born-Oppenheimer approach relies on the smallness of retardation effects. One way of quantifying retardation effects is to compare mass splittings as determined from the leading Born-Oppenheimer approximation with those determined from simulations. A Monte Carlo study with $\beta = 3.0$, $\xi = 3$ using a leading-order (but lattice-spacing corrected) nonrelativistic action for the heavy quark was performed. The effective masses for the two lowest-lying mesons in the exotic 1^{-+} channel are shown in Fig. 3. The comparison of mass splittings (for several quark-spin–restored states relative to the Υ) are shown in Table 2. All results are expressed in terms of

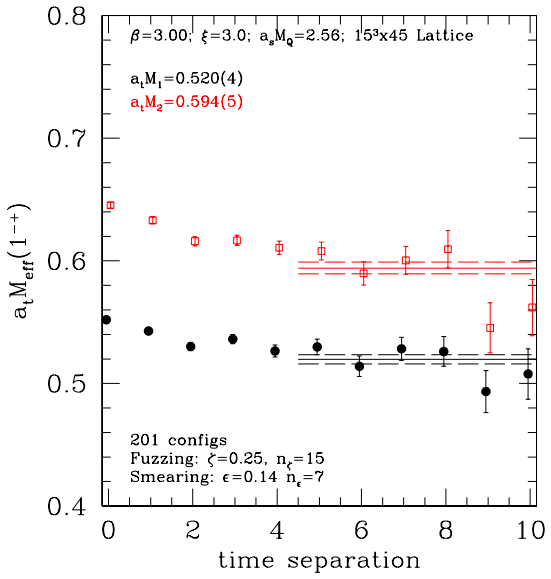

Figure 3. Effective mass plots for the two lowest-lying mesons in the exotic T_1^{-+} channel. Mass estimates from fitting the 2×2 correlator matrix elements using their expected asymptotic forms are shown. The heavy quark propagates according to a spin-independent nonrelativistic action.

the inverse hadronic scale r_0^{-1}. In the NRQCD simulations, the bare quark mass was taken to be $a_s M_b = 2.56$. The so-called kinetic mass of the Υ was then determined from its low-momentum dispersion relation. Half of this mass was used for the quark mass in the leading Born-Oppenheimer calculation. This ensured that the Υ kinetic masses were identical in both calculations. Assuming that the simulation results do not suffer significantly from lattice artifacts, one sees that retardation affects the spin-averaged mass splittings by less than 10%, validating the Born-Oppenheimer expansion.

5. Conclusion

The spectrum of gluon excitations in the presence of a static quark-antiquark pair was comprehensively surveyed for separations r ranging from 0.1 to 4 fm. Our results raised serious doubts on the validity of treating glue in terms of a fluctuating string for r less than 2 fm. For r between 2 and 4 fm, some tantalizing signatures of Goldstone mode formation were observed, but discrepancies still remain. We are currently studying the role of the spatial fixation or clamping of the quark and antiquark sources in distorting the Goldstone mode spectrum. Future studies of the excitation spectrum of the periodically-closed flux are planned. Lastly, retardation effects in quarkonium were found to be sufficiently small to validate the Born-Oppenheimer expansion.

Table 2
Comparison of meson mass splittings as determined from the leading Born-Oppenheimer approximation (LBO) and nonrelativistic simulations (NRQCD). The splittings are all taken relative to the mass of the Υ and are in terms of r_0^{-1}. The orbital angular momentum L and glue energy Γ assignments in the LBO for each level are indicated, along with the radial quantum number n. The size of the differences are listed as percentages of the simulation results.

	nL_Γ	NRQCD	LBO	Difference
χ_b	$1P_{\Sigma_g^+}$	0.96(1)	0.872(5)	9(1)%
Υ'	$2S_{\Sigma_g^+}$	1.30(1)	1.224(3)	6(1)%
1^{-+}	$1P_{\Pi_u}$	3.29(5)	3.166(3)	4(2)%
$1'^{-+}$	$2P_{\Pi_u}$	4.20(7)	3.772(2)	10(2)%
0^{+-}	$1P_{\Pi_u}$	3.51(8)	3.166(3)	10(2)%
0^{*++}	$1S_{\Sigma_u^-}$	3.56(8)	3.807(12)	7(2)%

This work was supported by the U.S. DOE, Grant No. DE-FG03-97ER40546.

REFERENCES

1. S. Perantonis and C. Michael, Nucl. Phys. **B 347**, 854 (1990); I.J. Ford, R.H. Dalitz, and J. Hoek, Phys. Lett. B **208**, 286 (1988); N. Campbell *et al.*, Phys. Lett. B **142**, 291 (1984).
2. K.J. Juge, J. Kuti, and C. Morningstar, Nucl. Phys. B (Proc. Suppl.) **63**, 326 (1998).
3. P. Hasenfratz, R. Horgan, J. Kuti, J. Richard, Phys. Lett. B **95**, 299 (1980).
4. C. Morningstar and M. Peardon, Phys. Rev. D **56**, 4043 (1997).

5. G. Bali, in preparation.
6. C. Michael, hep-ph/9809211.